Earthq Eng & Eng Vib (2025) 24: 101-112 **DOI**: https://10.1007/s11803-025-2290-z

Rapid post-earthquake safety assessment of low-rise reinforced concrete structures

Koji Tsuchimoto[1†], Yasutaka Narazaki[2‡] and Billie F. Spencer, Jr.[3§]

1. *International Design Division, Design Department, Taisei Corporation, Tokyo 163-0606, Japan*
2. *Zhejiang University – University of Illinois Urbana-Champaign Institute, Zhejiang University, Haining 314400, China*
3. *Civil and Environmental Engineering, University of Illinois Urbana-Champaign, Urbana 61821, USA*

Abstract: Many countries throughout the world have experienced large earthquakes, which cause building damage or collapse. After such earthquakes, structures must be inspected rapidly to judge whether they are safe to reoccupy. To facilitate the inspection process, the authors previously developed a rapid building safety assessment system using sparse acceleration measurements for steel framed buildings. The proposed system modeled nonlinearity in the measurement data using a calibrated simplified lumped-mass model and convolutional neural networks (CNNs), based on which the building-level damage index was estimated rapidly after earthquakes. The proposed system was validated for a nonlinear 3D numerical model of a five-story steel building, and later for a large-scale specimen of an 18-story building in Japan tested on the E-Defense shaking table. However, the applicability of the safety assessment system for reinforced concrete (RC) structures with complex hysteretic material nonlinearity has yet to be explored; the previous approach based on a simplified lumped-mass model with a Bouc-Wen hysteretic model does not accurately represent the inherent nonlinear behavior and resulting damage states of RC structures. This study extends the rapid building safety assessment system to low-rise RC moment resisting frame structures representing typical residential apartments in Japan. First, a safety classification for RC structures based on a damage index consistent with the current state of practice is defined. Then, a 3D nonlinear numerical model of a two-story moment frame structure is created. A simplified lumped-mass nonlinear model is developed and calibrated using the 3D model, incorporating the Takeda degradation model for the RC material nonlinearity. This model is used to simulate the seismic response and associated damage sensitive features (*DSF*) for random ground motion. The resulting database of responses is used to train a convolutional neural network (CNN) that performs rapid safety assessment. The developed system is validated using the 3D nonlinear analysis model subjected to historical earthquakes. The results indicate the applicability of the proposed system for RC structures following seismic events.

Keywords: rapid post-earthquake safety assessment; acceleration; interstory drift angle; damage sensitive feature; convolutional neural network; RC structure; simplified non-linear analysis model; Takeda degradation model

1 Introduction

Civil infrastructure currently plays an important role in the service of society; much of this infrastructure, including buildings, bridges, and lifeline systems, was constructed decades ago. After an earthquake occurs, such structures may suffer from damage or collapse (Midorikawa *et al*., 2011; Takewaki *et al*., 2011; Shirahama *et al*., 2016), and rehabilitation is an urgent matter for resumption of operation. The rehabilitation process begins with structural condition assessment, usually by field investigation, which is traditionally conducted by experts (certified structural engineers). After field inspection occurs, guidelines (e.g., JBDPA, 2023; ATC-20-1, 2005) are followed to categorize the building into three safety levels: inspected, restricted use, and unsafe. However, this process requires certified experts and is known to be time-consuming, dangerous, and subjective. In addition, the number of certified experts in Japan is insufficient for rapidly inspecting all buildings in urban area, necessitating a system to rapidly evaluate the safety of structures after seismic events. Therefore, an automated rapid post-earthquake safety assessment system is required to minimize the impact to human lives and business operations.

Structural health monitoring (SHM) provides a quantitative understanding of the current structural condition using measured data, such as accelerations and interstory drift angles. SHM can also reduce periodic maintenance/inspection time and cost (Mita *et al*., 2016; Xu and Mita, 2021). Some researchers have applied computer vision techniques to improve

Correspondence to: Koji Tsuchimoto, International Design Division, Design Department, Taisei Corporation, Tokyo 163-0606, Japan
Tel.: +81-8051885965
Email: tuchy0212@gmail.com
[†]Senior Engineer; [‡]Assistant Professor; [§]Professor
Received July 1, 2023; **Accepted** July 19, 2024

field inspections. For example, Narazaki *et al.* (2019, 2020, 2022) proposed an approach for vision-based autonomous navigation planning of unmanned aerial vehicles (UAVs) to collect images and automatically localize critical structural components to assist in the inspection process. The validation was conducted in a synthetic environment representing Japanese high-speed railway viaducts. Hoskere *et al.* (2017, 2020) suggested a new damage localization and classification technique for six different types of destruction: concrete cracks, concrete spalling, exposed reinforcement rebars, steel corrosion, steel fractures, and fatigue cracks. By training for various types of damage, this system can identify damage found in exposed structural components. These approaches have great potential for structural components that are externally exposed, such as bridges and external walls of buildings. However, applying this system to buildings is not straightforward, because not all structural components are visible from the outside (for example, beams inside of ceilings and columns covered by various types of finishing).

Vibration-based SHM has been widely recognized as an approach for identifying structural damage that may not be visible externally, and its level of sophistication and practicality is accelerating significantly with the advances in machine learning or deep learning techniques. Abasi *et al.* (2021) proposed an approach for damage detection and localization of 3D structures based on the frequency response function (FRF), principal component analysis, and nearest neighbor search method. The proposed approach was verified by an experimental test using aluminum columns and stainless slabs fixed by bolts. The efficacy of the proposed method was shown by a comparison with the artificial neural network-based damage detection method. By providing different levels of white Gaussian noise to obtain the FRF, the robustness of this system was also evaluated. The results indicated that the proposed method has high performance to detect damage location and condition with high accuracy against noisy data. Chegeni *et al.* (2022) introduced supervised learning classifiers to locate and quantify single and multiple damage scenarios. Auto regressive (AR) modeling was applied to extract time-series features for damage detection. Structural damage conditions are then assessed by calculating indices, such as coefficient relative error index (CRI) and residual relative error index (RRI) using coefficients and residuals of the AR models. Verification of this proposed approach was conducted using experimental datasets of a laboratory frame structure and a four-story ASCE benchmark structure, showing successful damage localization and quantification results. However, reinforced concrete structures subjected to seismic excitations exhibit significantly more complex nonlinear behaviors (e.g., nonlinearity may not always be attributed to damage, and such behavior changes significantly depending on structural systems and excitation levels); approaches based on the detection of deviation from linear models do not necessarily lead to accurate damage assessment results.

Characterization of nonlinear structural behavior during earthquakes is a promising approach to making rapid post-earthquake safety assessment of complex civil structures. Tsuchimoto *et al*. (2021a) developed an approach for building safety classification using sparse acceleration measurements. The building safety classification system estimates the maximum interstory drift angle (*IDA*) from floor accelerations using convolutional neural networks (CNNs). The approach was first validated using a 3D nonlinear analysis model of a five-story steel building. Subsequently, Tsuchimoto *et al.* (2021b) experimentally validated the approach using data from shake table tests carried out at E-Defense for a 1/3-scale, 18-story experimental steel structure that is representative of Japanese office buildings (Suita *et al*., 2015). Not only was the feasibility of the proposed approach demonstrated, but the importance of model updating before calculating damage sensitive features (*DSF*s) was illustrated. To date, the validations have been limited to steel structures; the applicability has not yet been explored for RC structures, which is particularly common for residential buildings due to the necessity for stiffness and high sound insulation performance. Compared to steel structures, seismic modeling of RC structures is significantly more challenging due to complex hysteretic material nonlinearity caused by cracking and rebar yielding. Therefore, additional investigation and validation are required to extend such rapid safety assessment framework to RC structures.

This study investigates rapid post-earthquake safety assessment of low-rise RC structures by using sparse acceleration measurements. Low-rise RC structures are commonly constructed in Japan for residential buildings due to high performance against wind loading, sound insulation, and fire resistance (Iizuka, 2013). The Statistics Bureau of Japan (2008) showed that the number of residential buildings with one to two stories accounts for 27.6% of the total building inventory, and approximately 41.1% of those buildings are RC structures. In addition, many researchers (Niraj and Anil, 2022; Feng *et al*., 2018) introduced low-rise RC moment frame structures to develop fundamental structural phenomena (e.g., collapse assessment, seismic energy dissipation). From these points of view, the system is developed and validated by employing a 3D nonlinear analysis model of a two-story low-rise RC building as a testbed. The importance of modeling the nonlinearity using a simplified model of RC structures from 3D nonlinear model is first discussed. Modal analysis and pushover analysis are conducted by utilizing the full 3D model to generate force-interstory drift angle curves to create a simplified lumped mass analysis model by use of the curve fitting method. Next, the training data for CNN-based *IDA* estimation is generated by using the simplified model. The trained CNN is employed to classify the building safety immediately following earthquakes. The approach is validated for the full 3D nonlinear model of the building, demonstrating the

feasibility of the rapid safety assessment of RC buildings in the aftermath of seismic events.

2 Post-earthquake safety assessment method for RC buildings

This section discusses the proposed approach for rapid safety assessment of RC buildings after seismic events. The approach for the safety assessment system is based on previous work done by the authors (Tsuchimoto *et al*., 2021a, 2021b), however, the following additional consideration should be included: (1) safety classification of RC structures based on damage index consistent with current state of practice, and (2) simplified nonlinear modeling incorporating hysteretic model of RC structures. The approach estimates the maximum *IDA* using *DSF*s by convolutional neural networks, which are used to determine building safety categories. For the convenience of the reader, this section first summarizes this rapid safety assessment system and then discusses its extension to RC structures, including an approach for simplifying a full 3D nonlinear model without losing representative nonlinear characteristics.

2.1 Procedure for rapid safety assessment

The approach for the rapid safety assessment of buildings considered herein is based on an appropriate definition of the structure's damage index (*DI*). The selected *DI* should offer precise distinctions between undamaged and damaged structures. Researchers reported that the maximum *IDA* is an effective criterion for classifying a structure's safety (Mita *et al*., 2016; Tsang *et al*., 2009). From this perspective, the maximum *IDA* is selected as the *DI* for the safety evaluation system.

$$DI = \max_j \left\{ \max_t \left(\theta_j(t) \right) \right\} \tag{1}$$

where $\theta_j(t) = d_j(t) / h_j$ is the time history of interstory drift angle, $d_j(t)$ is the time history of interstory drift, and h_j is the story height, each for the *j*th floor.

Safety classification is performed using the estimated *DI*. This classification determines whether the structure is still habitable or a prompt evacuation is needed. For the latter case, a detailed inspection and precise structural analysis is required prior to resuming the operation. Three categorical labels are used for the safety classification: (i) safe, (ii) restricted use, and (iii) unsafe. The Japan Structural Consultant Association (JSCA, 2018) has developed building condition categories based on structural types (e.g., RC, steel, wooden, etc.) and the type of seismic frame system (e.g., moment resisting frame, RC wall, steel braces, etc.). The classification of building conditions shown in Table 1 is chosen for the RC moment resisting frame structure in this study.

For this study, the safety classification for an RC moment resisting frame structure is determined as follows.

(1) Safe: $0 \le DI \le 0.0033$;

(2) Restricted use: $0.0033 < DI \le 0.01$;

(3) Unsafe: $DI > 0.01$.

The presence of damage in a structure following seismic events can be determined by a feature derived from measured response data (Tsuchimoto *et al.*, 2021a and 2021b). A *DSF* is a quantity that distinguishes damaged structures from undamaged ones. The authors proposed using the difference between measured and predicted accelerations calculated by a linear analysis model as the *DSF*, which is formally described as follows:

$$DSF_i(t) = \ddot{x}_i(t) = \ddot{x}_{i,\,\text{measured}}(t) - \ddot{x}_{i,\,\text{linear}}(t) \tag{2}$$

where $\ddot{x}_{i\text{measured}}(t)$ is the *i*th measured acceleration and $\ddot{x}_{i\text{linear}}(t)$ is the corresponding *i*th story acceleration predicted from the linear analysis model. This *DSF* and the ground acceleration are used to estimate the maximum *IDA*.

To uncover the complex relationship between *DSF*s and maximum *IDA*, a CNN is employed. The input to the CNN contains measured ground acceleration and *DSF*s taken from a limited number of sensor measurements. The CNN estimates a scalar value of the maximum *IDA*. Training data for the CNN is needed to estimate maximum *IDA* from various ground motions. A 3D nonlinear analysis model of an RC structure is then created from design drawings to compute the nonlinear seismic response (e.g., accelerations and deflections) to random excitations. To efficiently generate a large amount of training data, simplified lumped mass linear and nonlinear analysis models are developed to represent the linear and nonlinear characteristics of the 3D analysis model. A Monte Carlo simulation is performed to generate training data using linear and nonlinear analysis models with random excitations. The next section discusses the modeling of RC structures

Table 1 Building condition of the RC moment resisting frame system and maximum *IDA* (JSCA, 2018)

Building condition	No damage	Minor damage	Damage	Extreme damage
Maximum *IDA*	1/300	1/150	1/100	1/75
Repair	No need	Minor repair	Repair of crack (Small-scale)	Repair of crack (Large-scale)

with complexity of nonlinearity (e.g., cracking, rebar yielding), which are important for creating accurate training data.

2.2 Development of simplified lumped mass model for RC structures

This section discusses the efficient procedure to develop a simplified lumped mass analysis model from a 3D nonlinear model of an RC structure to save time to develop training data for safety assessment. Many researchers have reported modeling approaches for RC structures based on comparisons between testing data and the analysis model. Takeda *et al*. (1970) proposed a seismic response analysis model of RC structures that can represent continually changing stiffness and energy-absorbing characteristics. The applicability of the model was experimentally tested using specimens that were subjected to dynamic excitations. Results showed that the proposed force-displacement hysteresis model agreed with the measured responses at all levels of ground excitation to a reasonable degree.

Saiidi (1982) presented the nonlinear dynamic response of a simple RC structure, consisting of a foundation, a short column, and a short beam at the top by comparing five different hysteresis models (Takeda, elasto-plastic, bilinear, Clough, and Q-Hyst model). The Takeda model was concluded to be the most realistic model since it was developed based on the experimental studies. Response computed with elasto-plastic and bilinear models demonstrated poor correlation with the response computed with the Takeda model, indicating that using these models to determine nonlinear response of RC components is not suitable.

Other researchers (Kunnath *et al*., 1990; Pelliciari *et al*., 2020) discussed system identification approaches to determine the parameters of Bouc-Wen models for concrete structures. Kunnath *et al*. (1997) defined six parameters of the Bouc-Wen model that affect stiffness and strength-degrading characteristics and incorporated them into the simulation model. These six parameters were determined to match the experimental and simulation responses. Results showed that the identified Bouc-Wen hysteresis model can reproduce experimental results with reasonable accuracy. These studies demonstrate that the nonlinear hysteresis model for seismic response analysis must consider both stiffness and strength degradation as observed in the experimental results of RC structures.

The rapid post-earthquake safety assessment system for an RC structure requires the creation of 3D and simplified analysis models that can predict the structure's dynamic responses against random excitations. Using an accurate simplified model derived from the full 3D model, a large amount of seismic response data can be efficiently generated to train a CNN for maximum *IDA* estimation. Based on the success in modeling experimental RC structural behaviors found in existing research, the Takeda degrading model is adopted in this study to represent the nonlinear hysteresis behavior of a simplified lumped mass analysis model of RC structures.

3 Numerical testbed

This section provides a numerical example to validate the proposed rapid safety assessment approach. Herein, a two-story RC moment resisting frame structure is considered as discussed in the introduction to represent typical low-rise commercial and residential buildings in Japan. A 3D nonlinear analysis model is first developed to represent the as-built structure. Then, two simplified 2-DOF analysis models (linear and nonlinear stiffness) are created based on the results of a pushover analysis of the 3D nonlinear analysis model by use of the curve fitting method. The differences in responses of the linear and nonlinear analysis models are explored to demonstrate the efficacy of *DSF*s. Training data for the CNN is produced next, using a Monte Carlo simulation of the simplified 2-DOF nonlinear analysis model, thereby circumventing the use of the computationally expensive 3D model. An initial evaluation of this proposed approach is conducted by utilizing the simplified nonlinear model subjected to ground motions that were not considered during the training of the CNN. A confusion matrix is used to evaluate the accuracy of the proposed approach for safety evaluation. Finally, validation of this approach is performed using the results of the 3D nonlinear analysis model subjected to a historical earthquake.

3.1 Overview of a representative two-story RC building

A two-story RC moment resisting frame structure that is representative of residential buildings in Japan is investigated to develop and evaluate the proposed approach. This particular building is 7.2 m tall, with a rectangular plan of 12.0 m width and 6.0 m length. The structural frames are designed by using a simple RC moment resisting frame that consists of slabs, beams, and columns. Those structural components are adopted to resist the dead load and external loads (e.g., wind, earthquake, etc.). The location of columns and beams are balanced to match the centers of gravity and rigidity to eliminate eccentricity effects.

A detailed 3D nonlinear analysis model is first developed by utilizing SNAP nonlinear analysis software (Arata *et al*., 2012), which is commonly employed for seismic design in Japan (Fig. 1). In this software, bending moment and shear force are considered for beam frames; on the other hand, axial force, bending moment, and shear force are considered for column frames. Those frames are structurally designed based on Architectural Institute of Japan (AIJ) Standard for RC Structures (AIJ, 2018). Beams and columns are modeled as nonlinear frame elements with lumped plasticity at both ends, which represent cracking and yielding hinges. The plastic hinges follow a tri-linear restoring force with

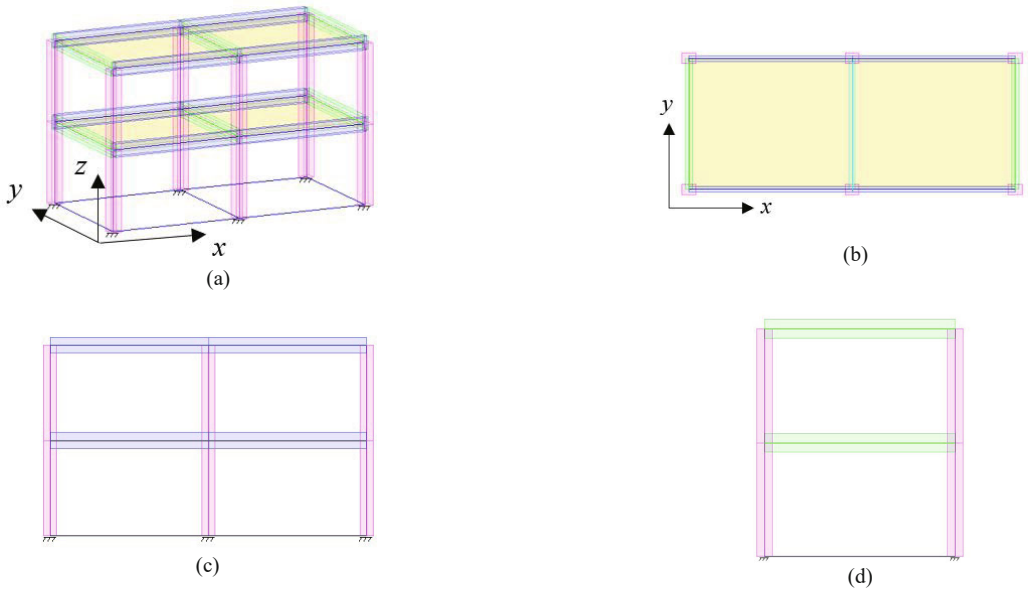

Fig. 1 Two-story building analysis model (3D model): (a) three-dimensional view; (b) plan view; (c) elevation view (*x*-axis); (d) elevation view (*y*-axis)

a stiffness degrading model. Beams are attributed as bending moment hinges. Columns take axial forces and form bending moment hinges defined by *M*-*N* interaction curves in both axes. Two floors are modeled as rigid bodies, whose motion is governed by the motion of a single node. Column bases are fixed, taking reactions for bending moments and shear forces. Modal analysis is conducted to identify the natural periods and mode shapes of the 3D model. Pushover analysis (Feng *et al.*, 2013) is then performed to obtain the static curve of the force-interstory drift angle plot of each story. Input lateral forces are applied to each story with a vertical triangle distribution pattern. Figure 2 shows the results of pushover analysis in the *x*-direction from the 3D nonlinear analysis model. These static curves are used to determine the simplified nonlinear model of each story (e.g., initial stiffness, restoring force characteristics).

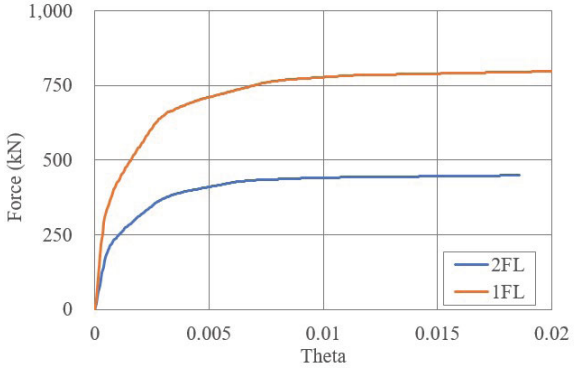

Fig. 2 Result of pushover analysis from 3D analysis model (*x*-axis)

3.2 Simplified lumped mass analysis model

Generating training data for CNN using a 3D nonlinear analysis model is computationally demanding. Therefore, this research uses simplified linear and nonlinear analysis models derived from the 3D analysis model to compute the structural response and the associated *DSF*s against random ground motions. The equation of motion for the *N*-degree of freedom structures with a simplified linear case is given by following second-order differential equations:

$$\boldsymbol{M}\ddot{\boldsymbol{u}} + \boldsymbol{C}\dot{\boldsymbol{u}} + \boldsymbol{K}\boldsymbol{u} = \boldsymbol{G}\boldsymbol{p}(t) \tag{3}$$

in which $\boldsymbol{M}$ is the mass matrix, $\boldsymbol{C}$ is the damping matrix, $\boldsymbol{K}$ is the stiffness matrix, and $\boldsymbol{u}$ is the displacement vector relative to the ground. Additionally, $\dot{\boldsymbol{u}}$, $\ddot{\boldsymbol{u}}$ are the corresponding velocity and acceleration vectors, $\boldsymbol{p}(t)$ is the input excitation vector, and $\boldsymbol{G}$ is the load effect matrix.

The simplified nonlinear static response of each story (*i*th story) is then incorporated into the lumped mass and shear spring model. To eliminate the effect of eccentricity, this simplified nonlinear analysis model is generated with a 2-DOF system (rotational degree is neglected). The shear spring at each story is modeled by a piecewise-linear curve with three stiffness coefficients, k_1, k_2, k_3 (Appendix A). The first breaking point in the curve indicates concrete cracking and second breaking point indicates rebar yielding. The coordinates of these points (P_{cr}, D_{cr}), (P_y, D_y) are determined from the pushover analysis results using the curve fitting method.

Pushover analysis results are used to determine the stiffness of the simplified linear and nonlinear models.

Among the parameters of the Takeda degrading model, cracking and yielding points are determined so that total energy dissipation during static loading is unchanged. Other parameters are manually adjusted to improve the match with the pushover curve. Mass and stiffness of the linear and nonlinear models is listed in Table 2. The static force-interstory drift angle curve of the simplified lumped mass analysis model is compared with the results of the pushover analysis of the 3D model in Fig. 3. Comparison of natural periods and mode shapes between 3D and simplified lumped mass analysis models are provided in Table 3 and Fig. 4, showing reasonable agreement.

Table 2 Parameters of the Takeda degrading model for the 2-DOF shear-beam model

Story *i*th	Floor height (m)	Mass	Stiffness		
		m_i (kN)	k_{1i} (kN/mm)	k_{2i} (kN/mm)	k_{3i} (kN/mm)
1	3.6	819	213.4	33.1	3.5
2	3.6	726	106.8	15.9	1.9

Table 3 Comparison of natural periods (*x*-axis)

Mode	3D model (s)	Simplified lumped mass model (s)
1st	0.218	0.218
2nd	0.063	0.094

3.3 Comparison of time history dynamic responses

The authors' preliminary investigation on an 18-story steel structure revealed that the accuracy of the simplified nonlinear model is important for obtaining accurate rapid post-earthquake safety evaluation results (Tsuchimoto *et al.*, 2021b). This section validates the accuracy of the simplified lumped mass analysis model using sinusoidal waves and data from historical earthquakes (El Centro NS). Time history data of acceleration and *IDA* is compared between the 3D model and the simplified lumped mass analysis models. Modal damping (1% damping in each mode) is added for both the 3D and simplified lumped mass analysis models.

Input excitations for this validation are shown in Fig. 5, and the maximum value, minimum value, and root mean square error (RMSE) of the acceleration and

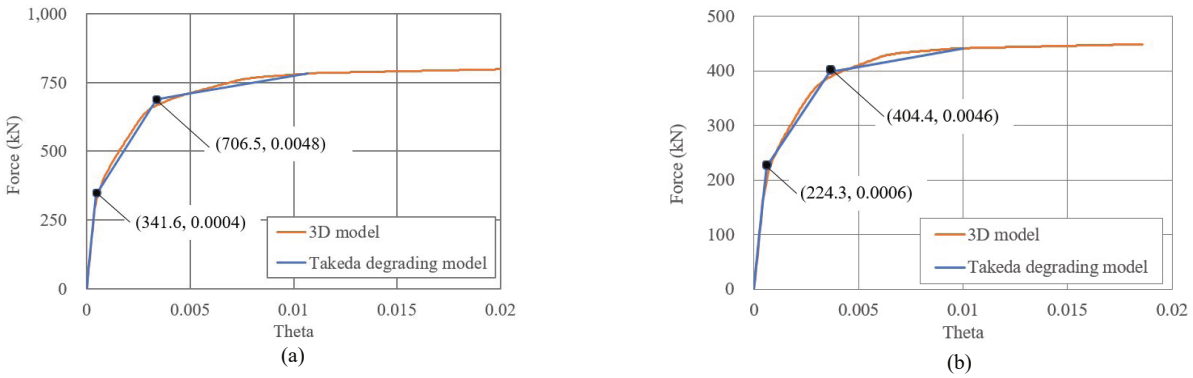

Fig. 3 Comparison of stiffness from the Takeda degrading model and pushover analysis results (*x*-axis): (a) 1st floor; (b) 2nd floor

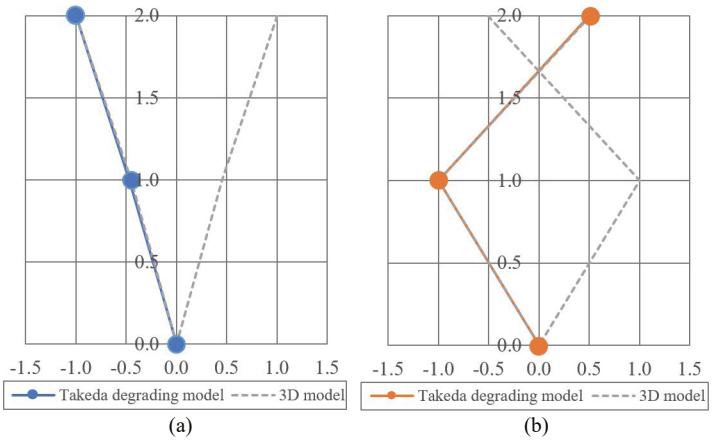

Fig. 4 Comparison of mode shapes (*x*-axis): (a) 1st mode; (b) 2nd mode

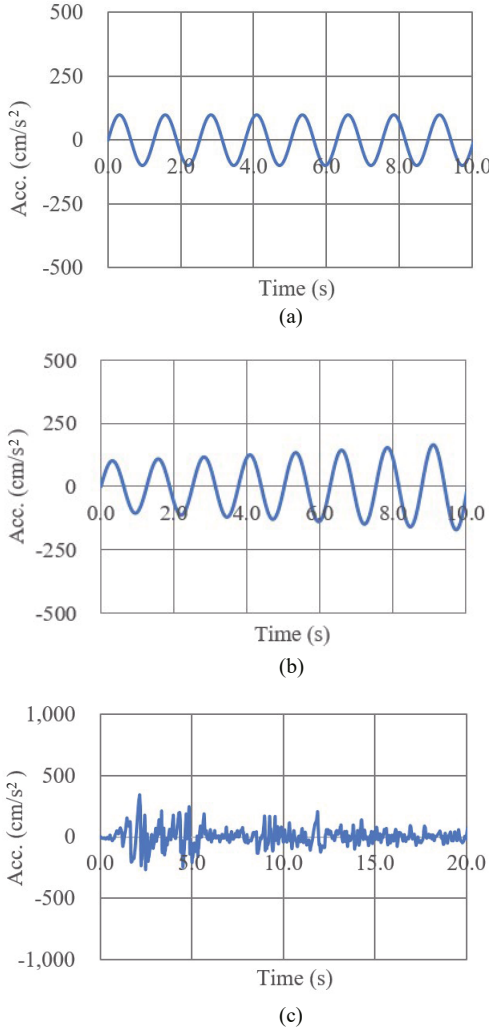

Fig. 5 Input excitations for time history dynamic responses (*x*-axis): (a) constant sine wave; (b) sine wave with gradually increasing amplitude; (c) El Centro NS

interstory drift angle for each of these excitations are shown in Table 4. Example comparisons of acceleration, interstory drift angle, and hysteresis behavior for El Centro NS excitation are provided in Figs. 6, 7, and 8. The results from the simplified model show a reasonable agreement with the results taken from the 3D analysis.

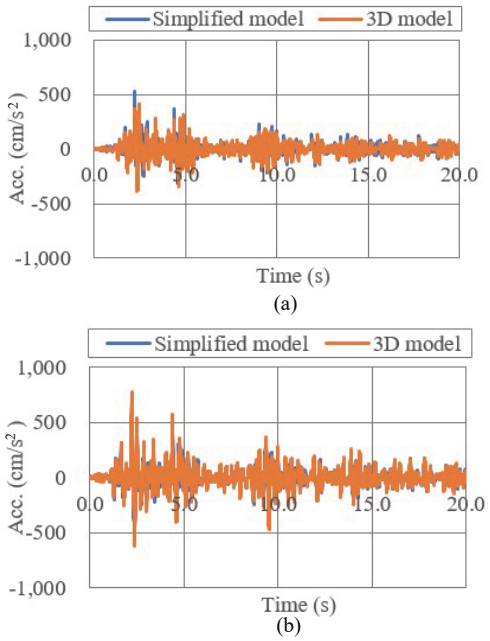

Fig. 6 Comparisons of accelerations for the El Centro NS excitation: (a) 1st floor; (b) 2nd floor

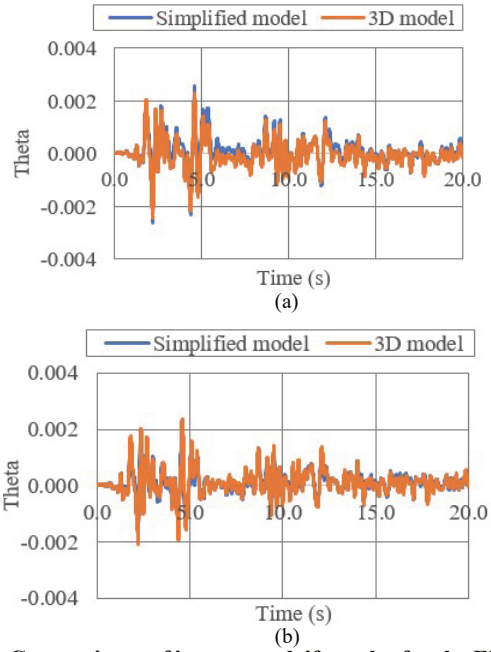

Fig. 7 Comparisons of interstory drift angles for the El Centro NS excitation: (a) 1st floor; (b) 2nd floor

Table 4 Comparison of maximum, minimum, and RMSE of acceleration and interstory drift angle for each of input excitations (*x*-axis)

		1FL						2FL					
		Acc. (mm/s²)			*IDA*			Acc. (mm/s²)			*IDA*		
		Max.	Min.	RMSE	Max.	Min.	RMSE	Max.	Min.	RMSE	Max.	Min.	RMSE
Sine1	3D	126.7	-104.1	17.0	2.3E-4	-2.2E-4	2.7E-11	243.7	-216.4	33.1	2.4E-4	-2.4E-4	1.3E-11
	Simp.	134.9	-106.8		2.3E-4	-2.3E-4		228.7	-214.3		2.3E-4	-2.3E-4	
Sine2	3D	127.3	-103.8	18.6	3.5E-4	-3.4E-4	4.0E-9	243.3	-217.7	46.1	3.6E-4	-3.5E-4	2.9E-9
	Simp.	130.4	-99.7		3.6E-4	-3.5E-4		230.0	-214.4		3.4E-4	-3.3E-4	
El Centro	3D	4064.7	-3909.6	625.3	2.3E-3	-2.4E-3	6.8E-8	7781.0	-6178.3	526.7	2.4E-3	-2.1E-3	2.2E-8
	Simp.	5235.9	-3442.3		2.6E-3	-2.6E-3		6099.4	-4605.4		1.9E-3	-1.6E-3	

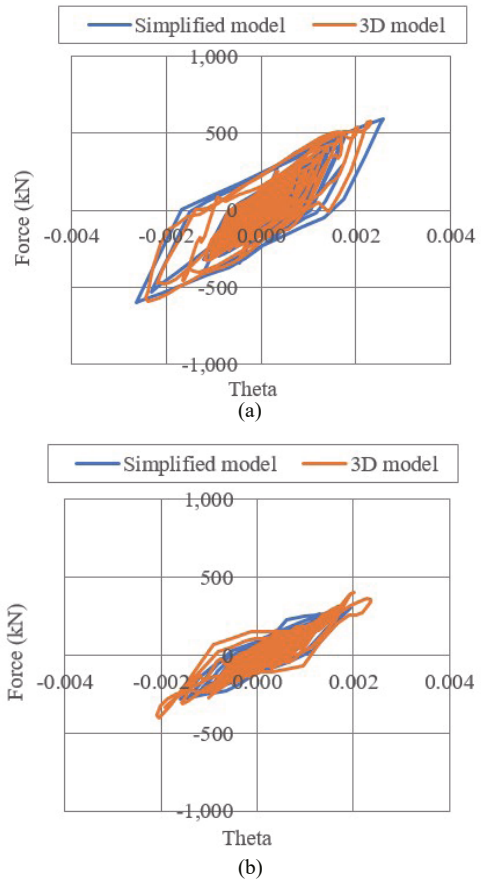

Fig. 8 Comparisons of hysteresis behaviors for the El Centro NS excitation: (a) 1st floor; (b) 2nd floor

3.4 Training of the convolutional neural network

A Monte Carlo simulation is conducted to generate a dataset for the CNN using the developed simplified nonlinear analysis model. Simulations are performed for a total of 80,000 ground excitations generated by filtering band limited white noise with the use of the Kanai-Tajimi spectrum. Each data sample consists of ground motion $\ddot{x}_g$ and the *DSF* of the 2nd floor, $\Delta\ddot{x}_2$, both of which contain 2,001 points with dt=0.02. The dataset is split into a training set (72,000 simulations) and a testing set (8,000 simulations).

The overall schematic architecture of the proposed CNN and the summary of each layer for the CNN structure are provided in Fig. 9 and Table 5, respectively. The CNN takes the time history of ground acceleration and the *DSF* of the 2nd floor and applies four convolutional layers in sequence. The output layer estimates the maximum interstory drift angle among all

Table 5 Summary of each hidden layer in CNN

Input layer	The size of inputs: 2 × 2,001 (Ground acceleration and 2nd floor DSF)
Convolutional layer	1st convolutional layer Learnable filter size: 2 × 10 The number of filters: 256 Stride: 1 Activation function: relu 2nd convolutional layer Learnable filter size: 1 × 10 The number of filters: 256 Stride: 1 Activation function: relu 3rd convolutional layer Learnable filter size: 1 × 10 The number of filters: 256 Stride: 1 Activation function: relu 4th convolutional layer Learnable filter size: 1 × 10 The number of filters: 256 Stride: 1 Activation function: relu
Pooling layer	Maximum pooling layer: 1 × 5
Fully connected layer	The number of connected layers: 2 layers The number of cells: 1,024 Activation function: relu
Output layer	The size of output: 1 (Maximum interstory drift angle of all floors)

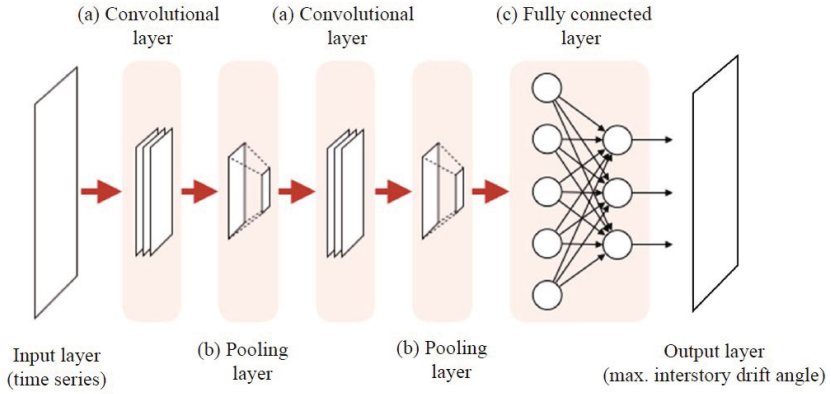

Fig. 9 Overall schematic of convolutional neural network (CNN)

floors, provided in Eq. (1). Following (Tsuchimoto *et al.*, 2021a), the model was trained by Adam optimizer (Kingma and Ba, 2014) for 160 epochs with batch size of 128. The learning rate was 0.001 during the first 100 epochs, and then reduced to 0.0001 and 0.00001 after the 100th and 150th epochs, respectively. A reverse Huber function is selected as a cost function of the training process (Laina *et al.*, 2016; Zwald and Lambert, 2012; Tsuchimoto *et al.*, 2021b). The decrease of the reverse Huber cost function indicates that the network converges (Fig. 10).

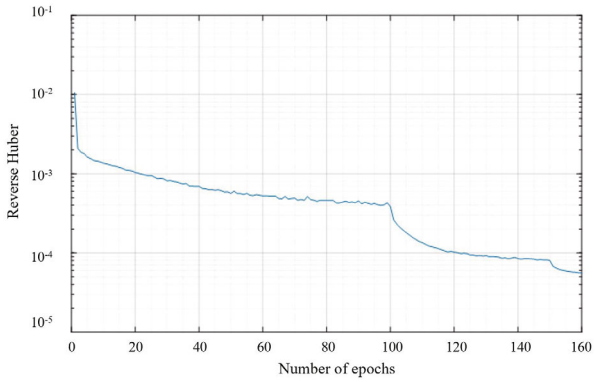

Fig. 10 Transition of cost function (reverse Huber) between prediction and true value

3.5 Evaluation of CNN

The performance of the CNN for maximum *IDA* estimation is evaluated by using a testing set consisting of 8,000 data samples. Acceleration response is estimated using a simplified nonlinear analysis model, and then the *DSF* at the 2nd floor is estimated by subtracting the response of the linear simplified model. Figure 11 illustrates the accuracy of the prediction by showing a scatter plot of prediction compared with true values. The plots will appear along the black line if predictions fit true values.

Based on the results shown in Fig. 14, the safety classification (provided in Table 1) is conducted to categorize the building into three safety levels, i.e., "safe" if the maximum *IDA* is less than 0.33%, "restricted use" if it falls between 0.33% and 1.0%, and "unsafe" if it is more than 1.0%. In this research, a "restricted use" zone

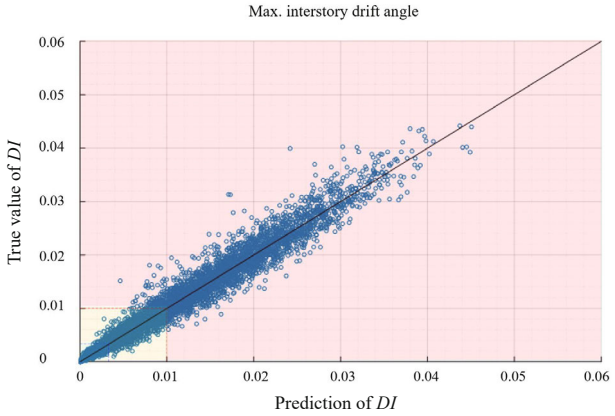

Fig. 11 Comparison between the predictions and true values for the maximum *IDA*

is separated into three regions: maximum *IDA* is less than 0.5%, between 0.5% and 0.67%, or larger than 0.67%. These additional categories help engineers assess a building's condition with a higher degree of confidence. The accuracy of these results is shown as a confusion matrix, displayed in Fig. 12. The proposed approach for an RC structure can estimate safety categories with 93.7% of accuracy, demonstrating a high potential of safety assessment following seismic events.

3.6 Validation results using 3D analysis model

This section validates the developed post-earthquake safety assessment system using acceleration response data taken from the 3D analysis model. The testing data is generated using historical earthquakes (El Centro NS) with 15 different peak ground accelerations (PGAs). The *DSF* at the 2nd floor is computed from the acceleration of the 3D model and acceleration predicted by the simplified lumped mass linear analysis model. Next, the ground acceleration and the 2nd floor *DSF* are fed into the trained CNN to estimate maximum *IDA*. Finally, safety classification is conducted using the estimation results.

The scatter plot in Fig. 13 shows a reasonable match between the predicted and true maximum *IDA*. A safety classification is then performed following the classification defined and shown in Table 1. The accuracy of the safety evaluation is presented in the

True value of *DI* \ Prediction of *DI*	Safe	Restricted Use (<1/200)	Restricted Use (<1/150)	Restricted Use	Unsafe
Safe (<1/300)	3286	112	9	0	0
Restricted Use (<1/200)	77	244	99	15	0
Restricted Use (<1/150)	8	80	173	101	2
Restricted Use	1	13	107	526	144
Unsafe	0	1	7	141	2854

Fig. 12 Safety evaluation results (confusion matrix)

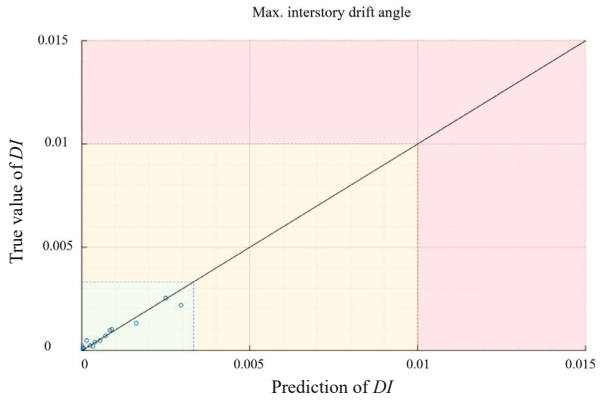

Fig. 13 Scatter plot between the predictions and true values, using accelerations from the 3D analysis model

form of a confusion matrix, as displayed in Fig. 14. The confusion matrix demonstrates that the trained CNN can estimate maximum *IDA* and classify the building condition with 100.0% accuracy for the considered historical earthquakes. These results demonstrate that the proposed approach can be utilized for the determination of building conditions for an RC structure.

4 Conclusions

The development and validation of an approach for rapid post-earthquake safety assessment of RC structures using sparse acceleration measurements is presented herein. A brief overview of the previous work done for the assessment of building conditions was presented, followed by discussions of the extensions to apply the system to RC moment resisting frame structures. This study selected the Takeda degrading model for RC nonlinearity, due to its successful modeling accuracy as reported in several existing experimental studies. A numerical example using a two-story RC structure was considered to validate the efficacy of the proposed approach. First, a detailed 3D nonlinear analysis model was created in SNAP nonlinear analysis software. Subsequently, simplified linear and nonlinear lumped mass models were developed to generate training data for the CNN-based maximum *IDA* estimation. Cracking and yielding points for the Takeda degrading model were determined through the use of pushover analysis results from the 3D nonlinear model, so that energy dissipation is equivalent between those two models. The modal analysis and time history analysis results of the simplified model with the identified Takeda degrading model were compared utilizing the results of the 3D analysis, showing reasonable agreement. The CNN was then trained using acceleration data and *DSF* data at the second floor as generated by simplified lumped mass linear and nonlinear models. The trained network showed 93.7% of accuracy. The system was further evaluated by using acceleration data from the 3D nonlinear model, subjected to a historical earthquake. The results showed that the proposed approach for rapid post-earthquake safety assessment for RC buildings can rapidly estimate safety conditions following seismic events with a high degree of accuracy.

Acknowledgement

The first author was supported by a fellowship from Design Department of Taisei Corporation; this generous support is gratefully acknowledged.

References

Abasi A, Harsij V and Soraghi A (2021), "Damage Detection of 3D Structures Using Nearest Neighbor Search Method," *Earthquake Engineering and Engineering Vibration*, **20**(3): 705–725.

AIJ (2018), *AIJ Standard for Structural Calculation of Reinforced Concrete Structures*, Architectural Institute of Japan.

Arata T, Hisada Y, Yamashita T and Kubo T (2012), "3-D Seismic Response Analysis of a High-Rise Building in Tokyo, Japan for the 2011 Tohoku Earthquake," *15th World Conference on Earthquake Engineering*, Lisbon, Portugal.

ATC-20-1 (2005), *Field Manual: Postearthquake Safety Evaluation of Buildings*, Applied Technical Council, Redwood, California, USA.

Chegeni MH, Sharbatdar MK, Mahjoub R and Raftari M (2022), "New Supervised Learning Classifiers for Structural Damage Diagnosis Using Time Series Features from a New Feature Extraction Technique," *Earthquake Engineering and Engineering Vibration*,

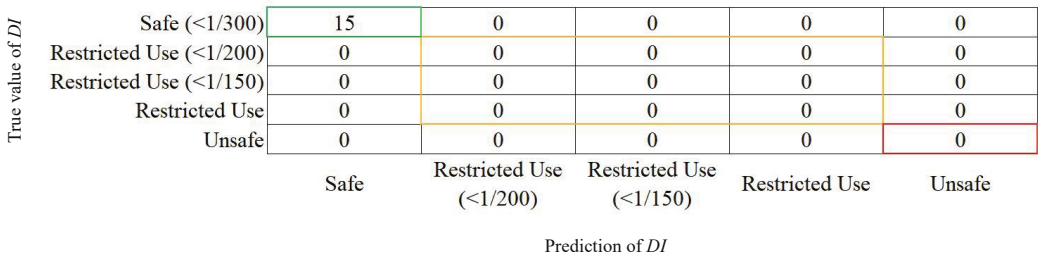

Fig. 14 Safety evaluation results (confusion matrix)

21(1): 169–191.

Feng D, Xia H, Kanamori S and Seki M (2013), "Design Comparison of the Seismically Isolated Building by the Chinese Code and Japanese Code, Part 2. Japanese Structural Design and Behavior to the Strong Ground Motions," *13th World Conference on Seismic Isolation, Energy Dissipation and Active Vibration Control of Structures*, Sendai, Japan.

Feng FF, Jiang KY, Huang HJ and Yi WJ (2018), "Earthquake Response of Low-Rise RC Moment Frame Structures According to Energy Dissipation Ratio of Beam-Column Joints," *Journal of Structural Integrity and Maintenance*, **3**(1): 33–43.

Hoskere V, Narazaki Y, Hoang TA and Spencer Jr. BF (2017), "Vision-Based Structural Inspection Using Multiscale Deep Convolutional Neural Network," *3rd Huixian Forum on Earthquake Engineering for Young Researchers*, Urbana, USA.

Hoskere V, Narazaki Y, Hoang TA and Spencer Jr. BF (2020), "MaDnet: Multi-task Semantic Segmentation of Multiple Types of Structural Materials and Damage in Images of Civil Infrastructure," *Civil Structural Health Monitoring*, **10**: 757–773.

Iizuka M (2013), "Design of Middle-to-Low-Rise Reinforced Concrete Structures (Focus on Residential Building)," *Concrete Engineering*, **51**(1): 63–67. (in Japanese)

JBDPA (2023), *Postearthquake Quick Inspection of Damaged Buildings*, The Japan Building Disaster Prevention Association, Online Available: http://www.kenchiku-bosai.or.jp/assoc/oq-index/, Accessed on 23rd of March, 2024.

JSCA (2018), *The Guide to Safe Buildings*, The Japan Structural Consultants Association, Japan.

Kingma DP and Ba J (2014), "Adam: A Method for Stochastic Optimization," *arXiv prepring arXiv*, **1412**: 6980.

Kunnath SK, Mander JB and Fang L (1997), "Parameter Identification for Degrading and Pinched Hysteretic Structural Concrete Systems," *Engineering Structures*, **19**(3): 224–232.

Kunnath SK, Reinhorn AM and Park YJ (1990), "Analytical Modeling of Inelastic Seismic Response of RC Structures," *Journal of Structural Engineering*, **116**(4): 996–1017.

Laina I, Rupprecht C, Belagiannis V, Tombari F and Navab N (2016), "Deeper Depth Prediction with Fully Convolutional Residual Networks," In *Proceedings of the 2016 Fourth International Conference on 3D Vision*, Stanford, CA, USA, pp. 239–248.

Midorikawa S, Ito Y and Miura H (2011), "Vulnerability Functions of Building Based on Damage Survey Data of Earthquakes After the 1995 Kobe Earthquake," *Journal of Japan Association for Earthquake Engineering*, **11**(4): 34–47.

Mita A, Hirai K and Ozawa S (2016), "Design Strategy of Structural Health Monitoring System Consisting of Four Sensors for Tall Buildings," In *Proceedings of the 8th European Workshop on Structural Health Monitoring*, Bilbao, Spain.

Narazaki Y, Hoskere V, Chowdhary G and Spencer Jr. BF (2022), "Vision-Based Navigation Planning for Autonomous Post-Earthquake Inspection of Reinforced Concrete Railway Viaducts Using Unmanned Aerial Vehicles," *Automation in Construction*, **137**: 104214.

Narazaki Y, Hoskere V, Eick B, Smith A and Spencer Jr. BF (2019), "Vision-Based Dense Displacement and Strain Estimation of Miter Gates with the Performance Evaluation Using Physics-Based Graphics Models," *Smart Structures and Systems*, **24**(6): 709–721.

Narazaki Y, Hoskere V, Hoang V, Fujino A, Sakurai Y and Spencer Jr. BF (2020), "Vision-Based Automated Bridge Component Recognition with High-Level Scene Consistency," *Computer-Aided Civil and Infrastructure Engineering*, **35**(5): 465–482.

Niraj M and Anil CW (2022), "Collapse Assessment of Low-Rise Reinforced Concrete Special Moment Resisting Frame Systems Using a Simplified Method," *Structures*, **38**: 1–13.

Pelliciari M, Briseghella B, Tondolo F, Veneziano L, Nuti C, Greco R and Tarantino AM (2020), "A Degrading Bouc-Wen Model for the Hysteresis of Reinforced Concrete Structural Elements," *Structure and Infrastructure Engineering*, **16**(7): 917–930.

Saiidi M (1982), "Hysteresis Models for Reinforced Concrete," *Journal of the Structural Division*, **108**(5): 1077–1087.

Shirahama Y, Yoshimi M, Awata Y, Maruyama T, Azuma T, Miyashita Y, Mori H, Imanishi K, Takeda N, Ochi T, Otsubo M, Asahina D and Miyakaua A (2016), "Characteristics of the Surface Ruptures Associated with the 2016 Kumamoto Earthquake Sequence, Central Kyushu, Japan," *Earth, Planets and Space*, **68**(1): 1–12.

Static Bureau of Japan (2008), *Commentary of Land Statistics Investigation in 2008: 2-1 Type of Residence, Construction, and Structure*, Online Available: https://www.stat.go.jp/data/jyutaku/2008/nihon/2_1.html, Accessed on 23rd of March, 2024.

Suita K, Suzuki Y and Takahashi M (2015), "Collapse Behavior of an 18-Story Steel Moment Frame During a Shaking Table Test," *International Journal of High-Rise Buildings*, **4**(3): 171–180.

Takeda T, Sozen MA and Nielsen NN (1970), "Reinforce Concrete Response to Simulated Earthquakes," *Journal of the Structural Division*, **96**(12): 2557–2573.

Takewaki I, Murakami S, Fujita K, Yoshitomi S and Tsuji M (2011), "The 2011 off the Pacific Coast of Tohoku Earthquake and Response of High-Rise Buildings Under Long-Period Ground Motions," *Soil Dynamics and Earthquake Engineering*, **31**: 1511–1528.

Tsang HH, Su R and Lam NTK (2009), "Rapid Assessment of Seismic Demand in Existing Building Structures," *The Structural Design of Tall and Special Buildings*, **18**(4): 427–439.

Tsuchimoto K, Narazaki Y, Hoskere V and Spencer Jr. BF (2021a), "Rapid Postearthquake Safety Evaluation of Buildings Using Sparse Acceleration Measurements," *Structural Health Monitoring*, **20**(4): 1822–1840.

Tsuchimoto K, Narazaki Y and Spencer Jr. BF (2021b), "Development and Validation of a Post-Earthquake Safety Assessment System for High-Rise Buildings Sing Acceleration Measurements," *Mathematics*, **9**(15): 1758.

Xu K and Mita A (2021), "Estimation of Maximum Drift of MDOF Shear Structures Using Only One Accelerometer," *Structural Health Monitoring*, **18**: 113–120.

Zwald L and Lambert LS (2012), "The BerHu Penalty and the Grouped Effect," *arXiv preprint arXiv*, **1207**: 6868.

Appendix A Schematic of modeling Takeda degrading hysteresis model

The simplified lumped mass analysis model in this research uses the Takeda degrading hysteresis model shown in Fig. A1. The nonlinear static response of the RC structure consists of three linear curves (k_{1i}, k_{2i}, k_{3i}), which are separated at the point of concrete cracking (P_{cr}, D_{cr}) and rebar yielding (P_y, D_y). Regarding case (b) in Fig. A1, the unloading stiffness is defined by using the following equation:

$$k_{ci} = \frac{|P| + P_{cr}}{|D| + D_{cr}} \tag{A1}$$

where k_{ci} is the unloading stiffness before the yielding point (P_y, D_y) at the ith story and (P, D) is the unloading force and deformation. After the structure reaches the zero-force state, the structure changes its slope and aims toward maximum (or minimum) experienced deformation. Regarding case (c) in Fig. A1, unloading stiffness k_{ri} is defined by following equation:

$$k_{ri} = k_y \left(\frac{D_y}{|D|} \right)^{0.4} \tag{A2}$$

where k_{ri} is the unloading stiffness after the yielding point (P_y, D_y) at the ith story, D is unloading deformation, and k_y is the stiffness, defined by following equation:

$$k_{yi} = \frac{P_y + P_{cr}}{D_y + D_{cr}} \tag{A3}$$

where (P_{cr}, D_{cr}), (P_y, D_y) are the cracking point and yielding point, respectively.

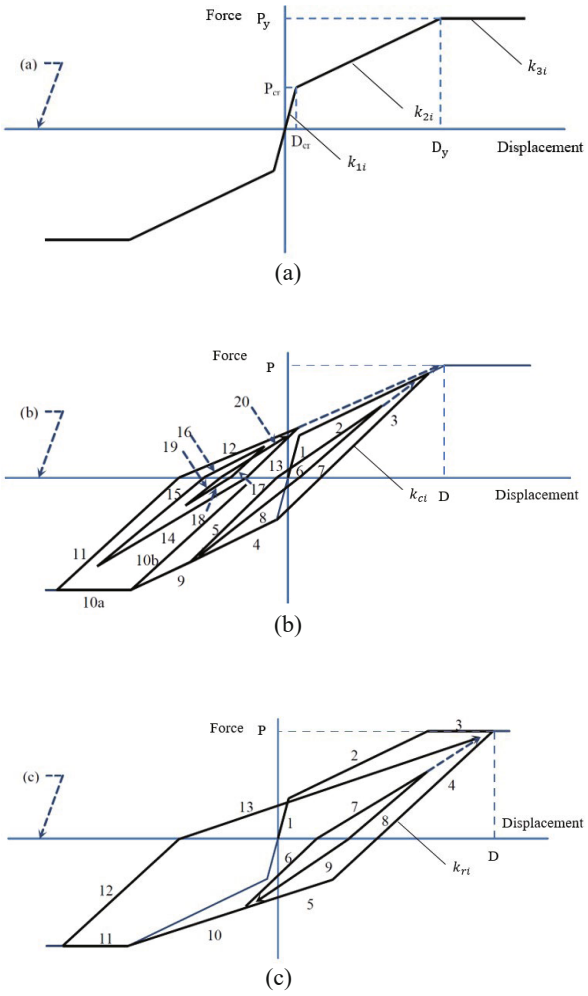

Fig. A1 Takeda degrading hysteresis model (Takeda *et al.*, 1970): (a) three-linear-stiffnesses of the *i*th story; (b) unloading stiffness before yielding; (c) unloading stiffness after yielding